IEEE Access
Multidisciplinary | Rapid Review | Open Access Journal

Received May 24, 2019, accepted June 12, 2019, date of publication June 20, 2019, date of current version July 17, 2019.

Digital Object Identifier 10.1109/ACCESS.2019.2924056

Fault Diagnosis of Circuit Breaker Energy Storage Mechanism Based on Current-Vibration Entropy Weight Characteristic and Grey Wolf Optimization–Support Vector Machine

SHUTAO ZHAO AND ERXU WANG
School of Electrical and Electronic Engineering, North China Electric Power University, Baoding 071003, China
State Key Laboratory of New Energy and Power Systems, North China Electric Power University, Baoding 071003, China

Corresponding author: Erxu Wang (946197703@qq.com)

This work was supported by the State Key Laboratory of New Energy and Power Systems.

ABSTRACT The reliable storage of spring potential energy is a prerequisite for ensuring the correct closing and opening operations of a circuit breaker. A fault identification method for circuit breaker energy storage mechanism, combined with the current–vibration signal entropy weight characteristic and grey wolf optimization-support vector machine (GWO-SVM), is proposed by analyzing the energy conversion and transmission relationship between control loop, motor, transmission component, and spring. First, the current envelope is denoised in the modulus maxima wavelet domain, the time-domain feature is extracted via a Hilbert transform (HT), and the kurtosis is calculated. Second, the energy method is used to select K parameters, the objective function optimization method is used to select α for variational mode decomposition (VMD), the intrinsic mode function (IMF) is obtained by decomposing the vibration signal with VMD and the permutation entropy characteristics of IMFs are extracted. Third, the characteristic of current and vibration signals for classification are edited by the entropy weight method, and the corresponding weights are provided in accordance with the sample information amount and importance. Finally, the current–vibration entropy weight characteristics are constructed and sent to the SVM model for learning and training. The GWO algorithm is used to optimize the parameters of the SVM model based on the mixed kernel function, which reduces adverse effects from the model parameters' choice of circuit breaker fault diagnosis. The results show that the overall diagnostic accuracy for the experimental samples reaches 100% and has good generalization capability based on the current–vibration entropy weight characteristic and the GWO-SVM method.

INDEX TERMS Current-vibration, entropy weight characteristic, grey wolf optimization–support vector machine (GWO–SVM), variational mode decomposition (VMD).

I. INTRODUCTION

The spring operating mechanism of the circuit breaker needs to sequentially control the energy storage motor, the gear transmission device, the spring energy storage medium, the stop plate and the limit switch before the opening and closing operation to realize the conversion, transmission and storage of the grid power to the spring mechanical energy. At present, the research on circuit breaker fault diagnosis mainly focuses on the process of opening and closing: using the control coil current, insulation rod displacement, vibration and sound signal to identify mechanical faults [1]–[3]. Many previous studies focus on solving problems in the operation of circuit breaker itself. However, the research on the failure of energy storage process is not deep enough, and there is no basis for quantitative evaluation of electric energy to mechanical energy conversion, transmission and storage process. Defects in any part of the energy storage will have an impact on the opening and closing operation of the circuit breaker. How to find the type of energy storage failure and

The associate editor coordinating the review of this manuscript and approving it for publication was Yu Wang.

the occurrence, development and change laws are worthy of further study.

The vibration signal is an important means to analyze the mechanical failure of the circuit breaker during operation, and it has important reference value for the fault diagnosis of the circuit breaker [4]. The main methods of vibration signal analysis include Dynamic Time Warping (DTW), Wavelet Transform (WT), Empirical Mode Decomposition (EMD)and Local Mean Decomposition(LMD) [5]–[8], but DTW is prone to distorting, the WT has energy leakage and the two cannot decompose the signal adaptively, and the EMD adaptive decomposition process is prone to generating end effect, modal aliasing, and envelope problems. LMD optimizes the problems of over-envelope and under-envelope of EMD. However, both LMD and EMD are recursive decomposition methods in essence, which can not fundamentally eliminate the endpoint effect and modal aliasing. Variational Mode Decomposition (VMD) is a new non-recursive mode decomposition method, which can effectively avoid the mode aliasing problem and has strong adaptability. It has a strong pertinence to the non-stationary vibration signals in the energy storage process of circuit breakers [9], [10].

The stator current signal is often used to diagnose the faults of the motor itself and its driving equipment. The working state of the mechanism is reflected by extracting the current signal characteristics [11]–[13]. The motor current signal in the energy storage process is accompanied by the vibration signal at the same time. So it can be considered to fuse the two signals together for circuit breaker diagnosis. Some scholars have studied the current-vibration signal and achieved good results [14].

The energy storage defects of circuit breakers can be diagnosed according to the characteristic changes of current envelope and vibration signals spectrum. How to quantitatively compare the characteristic differences of current-vibration signals is a key problem to be solved. The entropy weight method can measure the information dispersion degree in an indicator. It has been used to determine the weight of the fuzzy evaluation index that characterizes the insulator's pollution state and has achieved good diagnostic results [15]. The current and vibration signals in the energy storage process are fluctuating, and complex energy transfer makes the signal characteristics non-stationary. The introduction of the entropy weight method for the decision of feature vectors weight can avoid the error caused by subjective factors.

In view of the complex energy storage mechanism and energy storage control process of circuit breaker, power fluctuation, transmission mechanism jam, energy storage spring falling off and limit switch failures often occur, which lead to the failure of circuit breaker to complete the opening and closing operation normally. Therefore, data samples under the above circumstances are collected for research. SVM is used to classify and GWO is introduced to optimize the parameters, then verifies the accuracy and generalization of the model.

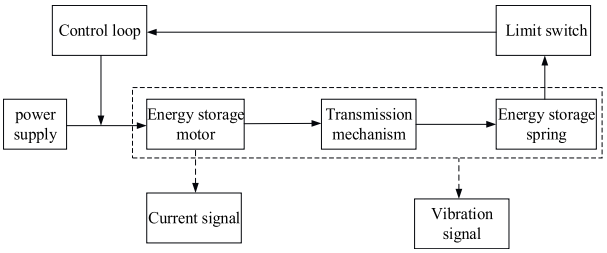

FIGURE 1. Energy storage mechanism monitoring diagram.

II. CIRCUIT BREAKER ENERGY STORAGE PROCESS AND FAULT DIAGNOSIS PROCESS

A. ENERGY STORAGE PROCESS AND SIGNAL MONITORING

The energy storage process of the circuit breaker of the spring operating mechanism: the power output is controlled after the power circuit is closed, and the electromagnetic torque generated by the energy storage motor acts on the transmission gearbox, and the energy storage spring is pulled up by the gear which changes the magnitude and direction of the torque, and the energy of switching on and off is stored. After the spring completes the energy storage, the limit switch operates and the control circuit cuts off the power supply. The motor voltage and torque equations for the circuit breaker energy storage process can be expressed as [16]:

$$u = Ri + L\frac{di}{dt} + Cw \tag{1}$$

$$Ci = J\frac{dw}{dt} + T_L + \beta w \tag{2}$$

where: u is the armature voltage, R is the armature resistance, i is the stator winding current, L is the armature inductance, w is the rotor angular velocity, C is the motor constant, J is the moment of inertia, T_L is the load torque, β is the rotational resistance coefficient.

It can be seen from equations (1) and (2) that the motor current signal is related to its own parameters and load torque. In the energy storage process, the mechanical components start, move and stop in strict accordance with a certain sequence, in electrical energy, mechanical energy, and spring energy storage, reflecting state changes.

When the energy storage control electrical circuit, mechanical motion and spring state change, the electrical topology and load torque are reflected in the motor current waveform directly or indirectly, and at the same time, a series of vibration signals superimposed by shock wave are generated along with the mechanism. These signal changes are closely related to the power supply, motor, transmission components, and spring compression process. Therefore, acquiring the current signals of energy storage motor and the vibration signals of energy storage mechanism can reflect its operation state. Fig.1 is the state signal acquisition schematic diagram of the circuit breaker energy storage mechanism.

The circuit breaker model used in the experiment is ZN65-12, rated voltage is 12 kV, energy storage motor model

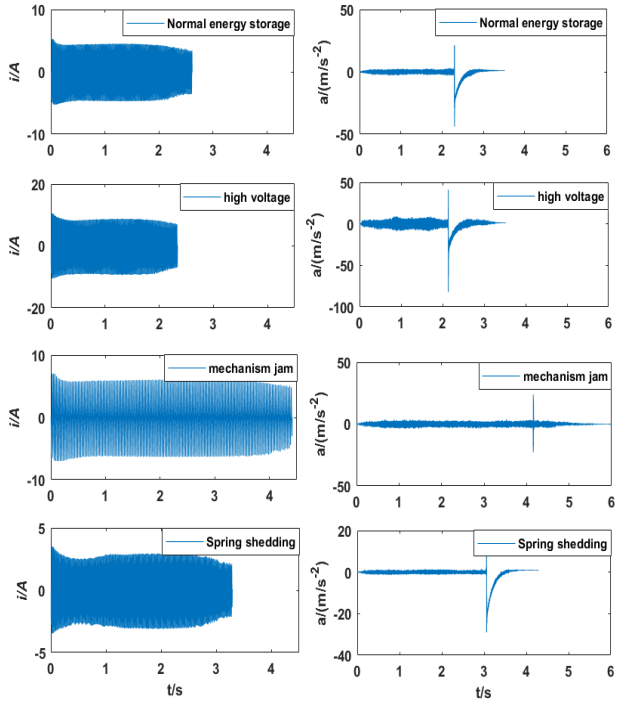

FIGURE 2. Current-vibration joint signal time-domain waveform.

is HDZ-22060B, rated voltage is 220 V, energy storage time under rated voltage is less than 10 seconds, DC resistance of opening and closing coil is 247Ω. Fig. 2 shows the motor current signal and vibration signal during normal energy storage state, power supply fluctuation (taking the high voltage as an example), mechanism jam and spring shedding state. It can be seen from the motor current signal of Fig. 2(a) that the normal energy storage time is about 2.5s. Compared with this: when the voltage is 120% of the rated voltage, the energy storage time is reduced, but the current amplitude is increased; the energy storage time of the mechanism jam and the spring shedding is obviously increased, and the energy storage time of the mechanism jam is the longest; The spring shedding causes the load torque to be reduced and the current amplitude is minimized. The vibration waveform of Fig. 2(b) shows a strong impact shock wave, and the normal energy storage is about 2.3s. Compared with this: when the voltage is too high that the vibration is drastic, the shock wave will appear in advance; the mechanism jam has the longest vibration duration and the vibration amplitude of spring shedding is the smallest and the shock wave is delayed.

In summary, the time domain current amplitude and its corresponding time characteristics are different under different working conditions, so that current envelope characteristics can reflect the change of energy storage state; the vibration signal waveform in time domain is more complex, so the feature vectors can be calculated from the frequency domain.

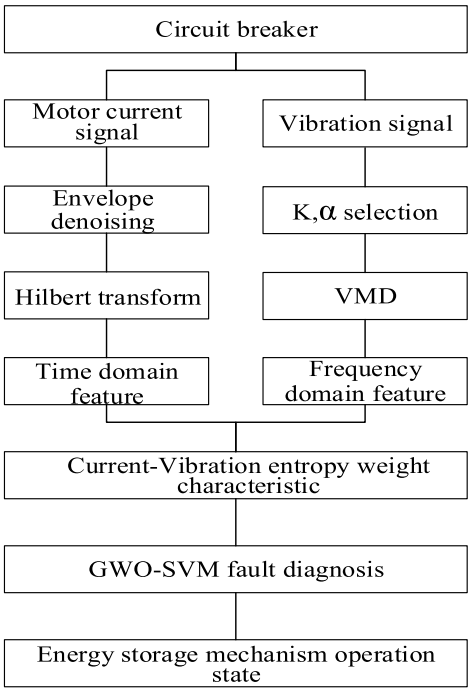

FIGURE 3. Flow chart of energy storage mechanism diagnosis.

B. FAULT DIAGNOSIS PROCEDURE FOR ENERGY STORAGE MECHANISM OF CIRCUIT BREAKER

The diagnosis process for the failure of the energy storage mechanism of the circuit breaker is proposed. Envelope de-noising in modulus maxima wavelet domain and HT are combined to obtain the time-domain characteristics of current signals. Energy method and objective function optimization method is used to get optimized parameters of VMD. Then extracting the frequency-domain characteristics of IMF components via VMD. The entropy weight method is used to combine the time-frequency characteristics of current-vibration signals. Then GWO-SVM is used to identify the operation state of energy storage mechanism, as shown in Fig. 3.

III. CURRENT-VIBRATION ENTROPY WEIGHT CHARACTERISTIC EXTRACTION

A. CURRENT SIGNAL FEATURE EXTRACTION IN TIME DOMAIN

In the process of energy storage, with the stretching of energy storage spring and the increase of load, there are many peaks of current signal in the process of motor running smoothly, and it is easy to be disturbed by white noise, which makes the envelope contour information extracted by HT demodulation very rough [17]. In order to extract the characteristics of current signal better, it is necessary to denoise the signal waveform envelope.

1) ENVELOPE DENOISING BASED ON MODULUS MAXIMUM WAVELET DOMAIN

Envelopes are processed by discrete wavelet transform, and get the wavelet coefficients set S(j, X_n)(j = 1, · · ·,J). Then,

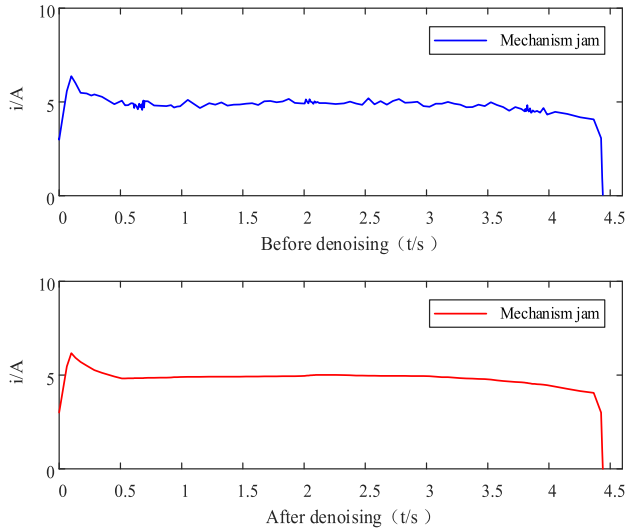

FIGURE 4. current envelope before and after denoising.

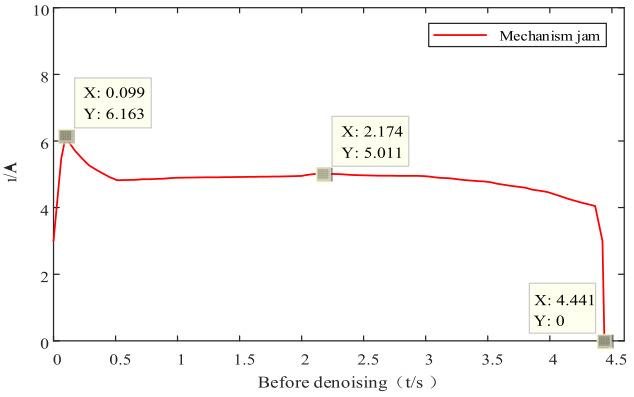

FIGURE 5. Energy storage mechanism stuck current envelope.

TABLE 1. Partial motor current characteristic.

Operating state	Group	Current characteristic					
		I_{st}	I_{sm}	T_{st}	T_{sm}	T_{tal}	K
normal	1	5.422	4.471	0.023	1.268	2.625	7.552
state	2	5.497	4.468	0.021	1.270	2.637	7.521
high	1	10.240	6.850	0.018	1.403	2.383	6.985
voltage	2	10.190	6.853	0.019	1.380	2.279	7.057
mechanism	1	6.163	5.011	0.099	2.174	4.441	7.935
jam	2	6.253	5.327	0.096	1.996	4.413	8.149
spring	1	5.110	3.758	0.014	1.334	2.719	9.266
shedding	2	5.085	3.770	0.014	1.314	2.719	8.996

the wavelet coefficients of each scale in S(j, X_n) are assigned to the maximum array MS(j, X_n), and the modulus maximum points of each scale in the array MS(j, X_n) are obtained by using Adhoc algorithm. The maximum point is reserved and the non-maximum point is set to zero. For two adjacent modulus extreme points X_k and X_l on two small scales, if the symbols are identical and the positions are close, X_l is considered as the breeding point of X_k, and the modulus extreme points of signals can be estimated from the breeding points. Assuming X_h as the extreme point of scale M, the method of determining the reproductive point of X_h in scale M-1 is as follows:

(1) Assuming that the extreme points before and after X_h are X_k and X_l respectively, and the corresponding reproductive point of X_k is X'_k, then the reproductive point of X_h is found on T = (max(X_k, X'_k),X_l).
(2) Points (I_1, I_2, ⋯, I_n) on T with the same symbol as X_h,if I_k satisfied $|I_k - X_h| \leq |I_i - X_h|/2$, ($i = 1, 2, \cdots, n$; $i \neq k$), it is the breeding site of X_h.
(3) If no such point exists, the point with the largest amplitude in the same sign point is the breeding point of X_h.
(4) If the amplitude is greater than $w \cdot X_h$ (w is constant, usually between 0.85 and 1.15), then X'_k and X_h will be the extreme points of noise and be removed, otherwise they will be retained.

According to the modulus maximum point in MS(j, X_n), the maximum point in the set of wavelet coefficients S(j, X_n) is determined. According to the definition of modulus maximum wavelet domain [18], the wavelet coefficients of the envelope are obtained, the wavelet coefficients of the noise are removed, and the purified envelope is obtained by the inverse transformation.

For the current envelope under energy storage mechanism jamming fault, before and after denoising, it is shown in Fig. 4.

Because of the interference of random noise, the extracted envelope contour is rough. As can be seen from the figure above, the denoising effect is obviously improved by using the modulus maximum wavelet domain denoising algorithm, and the clear and smooth signal envelope is obtained.

2) CURRENT CHARACTERISTICS EXTRACTION BY HT

The starting current, smooth running maximum current with the load and the cut-off current are key features that reflect the motor operating state.

As a dimensionless parameter, kurtosis is particularly sensitive to shock signals. It can be used to describe the peak degree of the current signal envelope that is activated or cut off, calculated as follows:

$$K = \frac{E(x-\mu)^2}{\sigma^4} \tag{3}$$

In the formula, $E(x)$ is the expected value of the current signal x, μ is the envelope mean and σ is the standard deviation.

Fig.5 is the current envelope of energy storage mechanism jam fault. It can be seen that the motor starting current I_{st} is 6.163A and the starting time T_{st} is 0.099s; the smooth running maximum current I_{sm} is 5.011A and the corresponding time T_{sm} is 2.174s; The total energy storage time T_{tal} is 4.441s, and the current envelope kurtosis value K is 7.935.

Partial current signals characteristics of energy storage motors under different operating conditions are shown in Table 1.

B. VIBRATION SIGNAL FEATURE EXTRACTION IN FREQUENCY DOMAIN

In different operating states of the circuit breaker energy storage mechanism, the time, amplitude and energy of the vibration shock wave will be different, which directly affects the frequency domain distribution of the signal.

1) VMD DECOMPOSITION PRINCIPLE

For signals of length N, $x(t) = \{x_1, x_2, \ldots, x_N\}$, whose VMD decomposition steps are as follows[19]:

The VMD decomposition mainly contains two parts: the establishment and solution of the variational constraint problem. The following problems are solved for the vibration signal with the data length N in the energy storage process:

$$\begin{cases} \min\limits_{\{u_k\},\{\omega_k\}} \left\{ \sum\limits_k \left\| \partial_t \left[\left(\delta(t) + \dfrac{j}{\pi t} \right) * \mu_k(t) \right] e^{-j\omega_k t} \right\|^2 \right\} \\ s.t. \ \sum\limits_k \mu_k = f \end{cases} \tag{4}$$

where:$\{\mu_p\} = \{\mu_1, \ldots, \mu_p\}$ is the decomposed P modes and $\{\omega_p\} = \{\omega_1, \ldots \omega_p\}$ is the center frequency of the P-th modes.

In order to find the optimal solution, the quadratic penalty factor α and the Lagrangian operator $\lambda(t)$ are introduced to change the constrained variational problem into a non-binding variational problem. The extended Lagrangian expression is:

$$\begin{aligned} &L(\{\mu_k\}, \{\omega_k\}, \lambda) \\ &= \alpha \sum_k \left\| \partial_t \left[\left(\delta(t) + \frac{j}{\pi t} \right) * \mu_k(t) \right] e^{-j\omega_k t} \right\|_2^2 \\ &\quad + \left\| f(t) - \sum_k \mu_k(t) \right\|_2^2 + \left\langle \lambda(t), f(t) - \sum_k \mu_k(t) \right\rangle \end{aligned} \tag{5}$$

The saddle point of equation (5) is solved by the alternate direction method of multipliers (ADMM), so that μ_k^{n+1}, ω_k^{n+1} and λ^{n+1} are continuously updated, and the modal component and center frequency are solved as follows:

$$\hat{\mu}_k^{n+1}(\omega) = \frac{\hat{f}(\omega) - \sum\limits_{i \neq k} \hat{\mu}_k^n(\omega) + \frac{\hat{\lambda}(\omega)}{2}}{1 + 2\alpha(\omega - \omega_k)^2} \tag{6}$$

$$\omega_k^{n+1} = \frac{\int_0^\infty \omega \left| \hat{\mu}_k^n(\omega) \right| d\omega}{\int_0^\infty \left| \hat{\mu}_k^n(\omega) \right| d\omega} \tag{7}$$

The VMD steps are as follows:

1) Initialize $\hat{\mu}_k^1$, ω_k^1, $\lambda^{\wedge 1}$ and n, let its initial value be 0, set the decomposition modal number K to 2, pre-decomposition optimization.
2) Update μ_k and w_k according to equations (6) and (7) respectively.
3) Update $\hat{\lambda}$

$$\hat{\lambda}^n(\omega) + \tau[\hat{f}(\omega) - \sum \hat{\mu}_k^{n+1}] \rightarrow \hat{\lambda}^{n+1}(\omega) \tag{8}$$

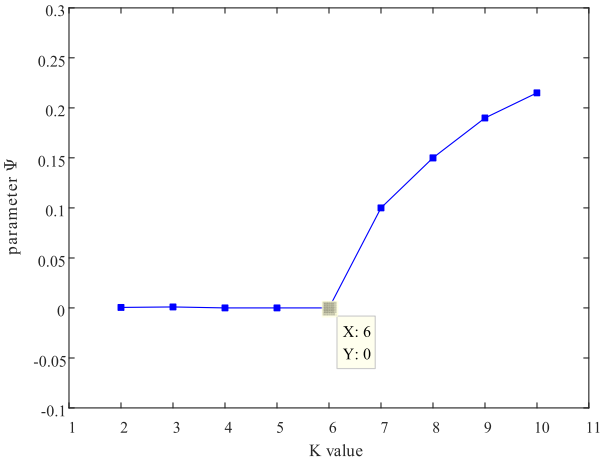

FIGURE 6. Change trend of K value.

4) If the following formula is satisfied, the iteration is stopped and the result is output; otherwise, it returns to step 2.

$$\sum \left\| \hat{\mu}_k^{n+1} - \hat{\mu}_k^n \right\|_2^2 / \left\| \hat{\mu}_k^n \right\|_2^2 < \varepsilon \tag{9}$$

2) VMD PARAMETER K OPTIMIZATION

In order to prevent the VMD from being over- decomposed, the K parameter is selected according to the energy conservation theory before and after decomposition. For the original vibration signal sequence $x(i)$, come from the energy storage mechanism, the energy calculation formula is as follows:

$$E = \sqrt{\frac{\sum\limits_{i=1}^{n} x^2(i)}{n}} \tag{10}$$

where: E represents the signal energy value and n is the number of sampling points. In order to characterize VMD's energy difference before and after the decomposition, the energy difference parameter ψ is defined and calculated as follows.

$$\psi = \frac{\left| \sum\limits_{x=1}^{K} E_x - E \right|}{E} \times 100\% \tag{11}$$

where: E_x corresponds to the energy of the x-th component, K is the number of components, and E is the original signal energy. Energy is conserved before and after decomposition (the ideal value of ψ is 0). After many experiments and calculations, the changing trend of K is shown in Fig.6:

The above figure shows that when K is greater than 6, the energy difference parameter ψ increases, and it can be judged that there is an over-decomposition phenomenon. The K value at the turning point is the optimal decomposition mode number of VMD.

3) VMD PARAMETER α OPTIMIZATION

The quadratic penalty factor α has a great influence on the accuracy of modal aliasing and reconstruction, so the

objective function is constructed by combining the density of modal aliasing and Pearson correlation coefficient. Then GWO is used to optimize the objective function to obtain the optimal parameter value α.

The frequency domain mode aliasing area (A) is defined as the sum of the same frequency amplitude overlap between adjacent modal center frequencies. The calculation steps are as follows:

$$A_k(\omega) = \begin{cases} |\mu f_i(w)| & |\mu f_i(w)| \le |\mu f_j(w)| \\ |\mu f_j(w)| & |\mu f_i(w)| > |\mu f_j(w)| \end{cases} \tag{12}$$

$$A = \sum_{\omega=m}^{n} A_k(\omega) \tag{13}$$

In the formula, $\mu f_i(\omega)$ and $\mu f_j(\omega)$ are frequency domain functions after Fourier transform of two adjacent modal functions $\mu_i(t)$ and $\mu_j(t)$, ω is frequency. $m = \min(\omega_i, \omega_j)$, $n = \max(\omega_i, \omega_j)$.

In order to quantitatively characterize the degree of modal aliasing between two adjacent IMFs, the frequency domain modal aliasing density (A_d) is defined. The calculation formula is as follows:

$$A_d = 1000\frac{A}{|\omega_i - \omega_j|} \tag{14}$$

The objective function is defined as the correlation coefficient between reconstructed signal and original signal divided by the frequency domain mode aliasing density. The formula is as follows:

$$\alpha_{obj} = A_d / \frac{\sum_{i=1}^{n}(x_i - \bar{x})(y_i - \bar{y})}{\sqrt{\sum_{i=1}^{n}(x_i - \bar{x})^2 \sum_{i=1}^{n}(y_i - \bar{y})^2}} \tag{15}$$

Set the initial value of α to 100 and use GWO to optimize the parameters. See sub-section A. GWO-SVM DIAGNOSTIC MODEL for the specific optimization process. The process of parameter optimization is as follows:

As can be seen from the Fig.7, with the increase of iteration steps, the value of objective function gradually decreases and converges. The final penalty factor α is 213.5.

After K and α are determined, the vibration signal under high energy storage voltage is decomposed, and the time-frequency diagram is shown in Fig. 8-9.

C. COMPUTING THE PERMUTATION ENTROPY OF MODAL COMPONENTS

1) PRINCIPLE OF PERMUTATION ENTROPY

Permutation entropy can detect sudden change points of signals, which has strong anti-noise ability and high time resolution. It has strong pertinence to non-stationary chaotic vibration signals in complex field environment of circuit breakers. The calculation steps are as follows [20]:

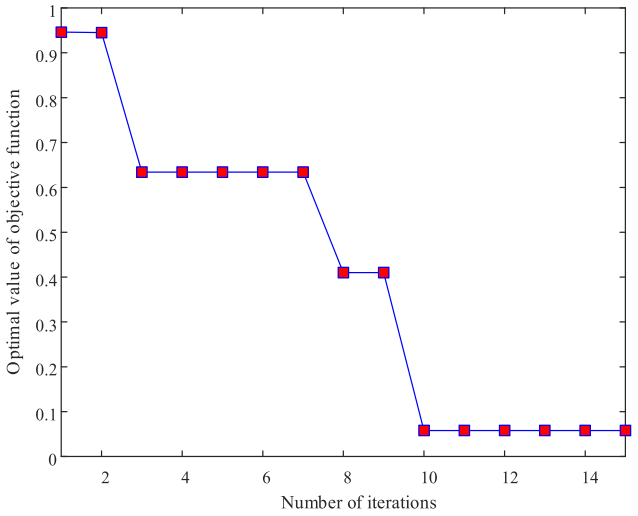

FIGURE 7. The α optimization process.

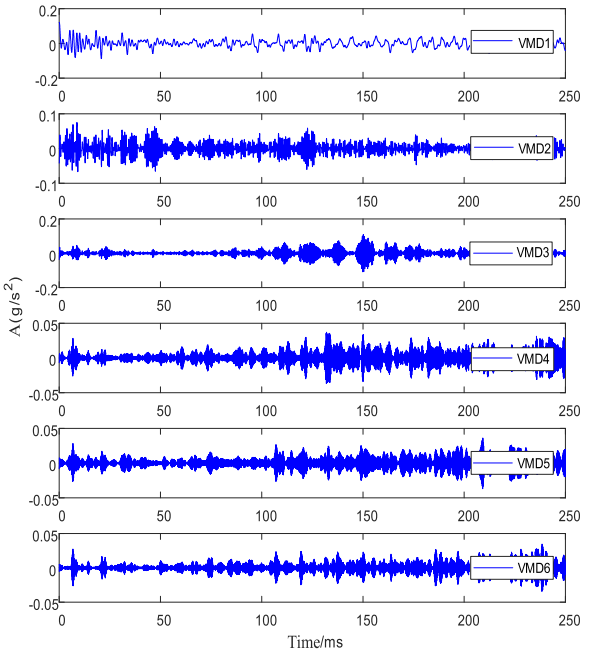

FIGURE 8. VMD decomposition in time domain.

For signal sequence $\{X(i), i = 1, 2, \cdots, n\}$, the phase space is reconstructed and the following matrix is obtained:

$$\begin{bmatrix} x(1) & x(1+\tau)\cdots x(1+(m-1)\tau) \\ x(2) & x(2+\tau)\cdots x(2+(m-1)\tau) \\ x(j) & x(j+\tau)\cdots x(j+(m-1)\tau) \\ \cdots & \cdots \\ x(k) & x(k+\tau)\cdots x(k+(m-1)\tau) \end{bmatrix} \tag{16}$$

where: j= 1, 2, ⋯, k, $k = n-(m-1)\tau$, m and τ is the embedded dimension and delay time. The elements of each component (k in total) are arranged in ascending order according to the numerical value, and different symbol sequences are obtained according to the reconstructed component index. The m-dimensional phase space mapping symbol sequence has $m!$ species, and the occurrence probability of s different symbol sequences are $P_1, P_2, \cdots, P_s$ respectively, calculated

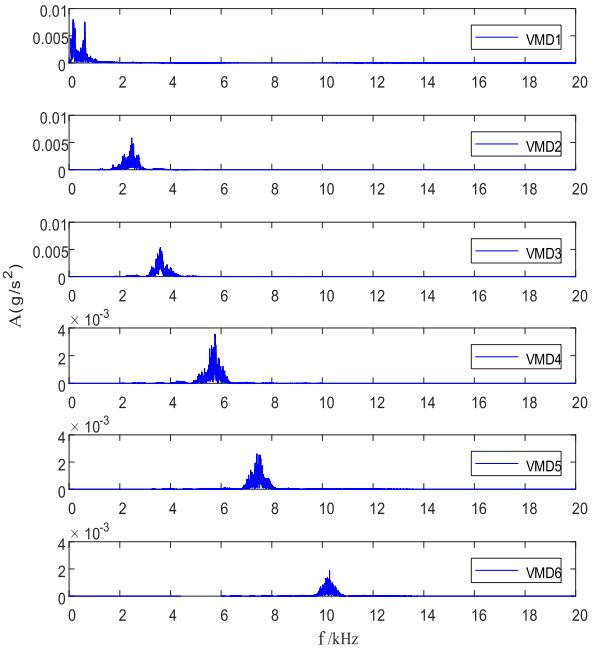

FIGURE 9. VMD decomposition in frequency domain.

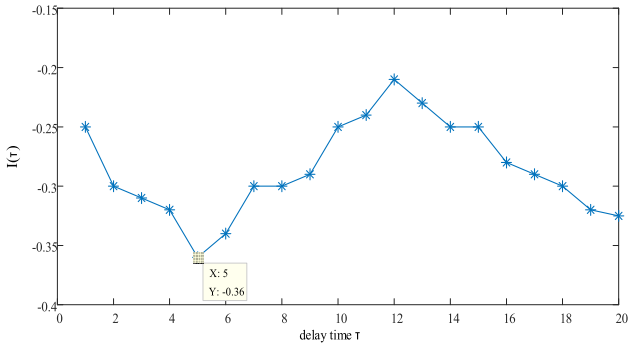

FIGURE 10. Curve of mutual information value changing with delay time.

as follows:

$$Pe(m) = -\sum_{j=1}^{s} P_j \ln P_j \tag{17}$$

2) SELECTION OF PARAMETER m AND τ

a: THE SELECTION OF DELAY TIME τ

Because the vibration signal of circuit breaker is non-linear, the mutual information method is chosen to calculate. See literature [21] for specific principles.

Record $I(\tau)$ as a function of τ, and select the first minimum point of $I(\tau)$ as the optimal delay time. The delay time curve of the vibration signal is shown in Fig.10.

As can be seen from the figure above, when τ is 5, the first minimum point appears, so this paper chooses the delay time as $\tau = 5$.

b: SELECTION OF EMBEDDING DIMENSION M

In order to ensure that the space can reproduce the original dynamic characteristics, the dimension of the embedded space should be large enough. In this paper, G-P algorithm is used, and the specific calculation steps are referred to reference [22]. R is the Euclidean distance between two points in phase space, and N(ε) is the correlation function. Draw the curve of ln(N(ε)) with respect to ln (R), as shown in Fig. 11.

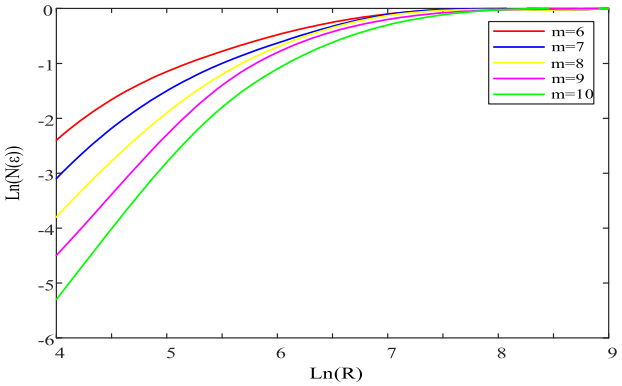

FIGURE 11. ln(N(ε)) curve along with ln(R).

TABLE 2. Partial vibration signal characteristics.

Operating state	Group	Vibration characteristics					
		P_1	P_2	P_3	P_4	P_5	P_6
normal	1	7.129	7.723	7.224	7.427	7.320	7.523
state	2	7.128	7.721	7.221	7.427	7.321	7.522
high	1	4.261	4.655	4.567	4.545	4.425	4.263
voltage	2	4.263	4.656	4.565	4.547	4.426	4.262
mechanism	1	5.788	5.466	5.135	5.635	5.885	5.359
jam	2	5.787	5.468	5.137	5.634	5.883	5.358
spring	1	2.235	2.528	2.728	2.523	2.356	2.182
shedding	2	2.236	2.529	2.723	2.524	2.352	2.183

Set D = ln(N(ε))/ln(R), The estimated value D(m_0) of correlation dimension corresponding to m_0 is obtained. Calculate the change rate of each curve in its approximate linear region. When m is 8, the D value is more stable and the corresponding curve linearity is better. So the embedding dimension m = 8 is chosen. After the parameters have been selected, the permutation entropy of the six modes of the vibration signal is obtained, as shown in Table 2.:

The value of permutation entropy is related to the rule degree of sample sequence. From Table 2., it can be seen that the difference of permutation entropy in different states is obvious, and it can be distinguished well. It can effectively characterize the state information of energy storage mechanism.

D. FEATURE VECTORS PROCESSING BASED ON ENTROPY WEIGHT METHOD

The entropy weight method can comprehensively evaluate the discreteness of the index characteristics. Considering the fluctuation of energy storage motor current and the non-stationary of the vibration signal, we introduce the entropy weight method to process the signal characteristic, and calculate the corresponding weight. It can avoid the error caused by subjective factors. The smaller the entropy is, the more information it contains, and vice versa [23].

Entropy weight method implementation process:

(1) Establish a feature vector matrix.
$A = \begin{pmatrix} X_{11} & \cdots & X_{1q} \\ \vdots & \vdots & \vdots \\ X_{p1} & \cdots & X_{pq} \end{pmatrix}$, where p is the four states of the above-mentioned circuit breaker energy storage; q refers to the dimension of the feature vector. X_{ij} refers to the j-th feature vector corresponding to the i-th state.

(2) Non-negative processing of data.
In order to avoid the meaninglessness of logarithm when entropy is obtained, the data needs to be non-negatively processed, so the data is translated and processed by the formula (18) and (19) according to the size of the characteristic value.

$$X'_{ij} = \frac{X_{ij} - \min(X_{1j}, X_{2j}, \cdots, X_{pj})}{\max(X_{1j}, X_{2j}, \cdots, X_{pj}) - \min(X_{1j}, X_{2j}, \cdots, X_{pj})} + 1, \quad i = 1, 2, \cdots p;\ j = 1, 2, \cdots, q \tag{18}$$

$$X''_{ij} = \frac{\max(X_{1j}, X_{2j}, \cdots, X_{pj})}{\max(X_{1j}, X_{2j}, \cdots, X_{pj}) - \min(X_{1j}, X_{2j}, \cdots, X_{pj})} + 1, \quad i = 1, 2, \cdots p;\ j = 1, 2, \cdots, q \tag{19}$$

(3) Calculate the index proportion of the i-th state in the j-th feature.

$$P_{ij} = \frac{X_{ij}}{\sum_{i=1}^{p} X_{ij}} \quad (j = 1, 2, \cdots, q) \tag{20}$$

(4) Calculate the entropy value of the j-th feature.

$$e_j = -k^* \sum_{i=1}^{p} P_{ij} \log(P_{ij}) \tag{21}$$

where $k > 0$, ln() is the natural logarithm, $e_j \geq 0$. The constant k in the equation is related to the energy storage state type of circuit breaker. General order $k = 1/\ln(p)$.

(5) Calculate the difference coefficient of the j-th feature.
For the j-th feature vector, the bigger the feature value X_{ij} difference is, the bigger the role of state evaluation is, the smaller the entropy value is. $g_j = 1\text{-}e_j$, then: the larger the g_j, the feature is more important.

(6) Weight coefficient.

$$W_j = \frac{g_j}{\sum_{j=1}^{p} g_j}, \quad j = 1, 2, \cdots, p \tag{22}$$

The corresponding weights are given according to the information quantity of the feature vectors. Table 3. shows the corresponding weights of the feature vectors under normal conditions.

The weight change in the four states of the circuit breaker energy storage process is shown in Fig. 12.

TABLE 3. Feature vectors weights in normal state.

Index	I_{st}	I_{sm}	T_{st}	T_{sm}	T_{tal}	K
weight	0.0594	0.0619	0.0913	0.0578	0.1424	0.0612
Index	P_1	P_2	P_3	P_4	P_5	P_6
weight	0.0877	0.1299	0.0975	0.0612	0.1363	0.0134

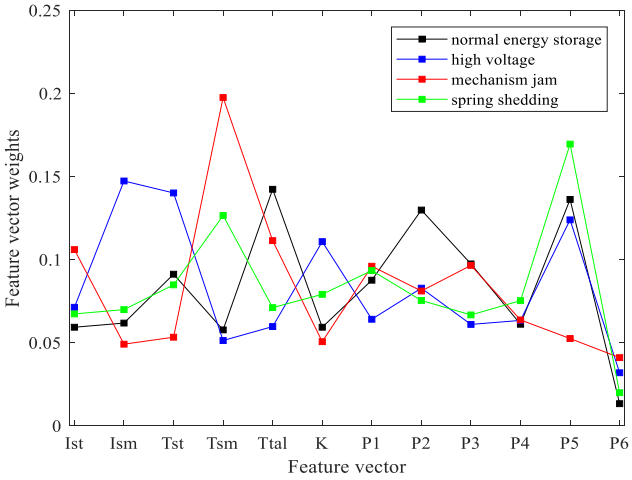

FIGURE 12. Feature vector weight in four states.

It can be seen from the weight change curve of Fig. 12 that the variation of each feature in the normal state is small, and the variation of each feature in the mechanism jam state is large. Among them, the smooth running maximum current and kurtosis in the mechanism jam state are small, and the smooth running maximum time is the largest. It can be seen that the entropy weight method distinguishes the feature vectors very well and can be used to construct the composite feature vectors of the current-vibration entropy weight feature.

IV. FAULT IDENTIFICATION OF ENERGY STORAGE MECHANISM BASED ON GWO-SVM

A. GWO-SVM DIAGNOSTIC MODEL

SVM has strong generalization ability and good convergence, which is especially suitable for small sample fault diagnosis. However, the selection of penalty factor C and kernel function type affects the classification performance of SVM directly. Considering that the samples in this paper are multi-sensor data feature sets, strong vibration and impact in energy storage process, and GA, PSO and other algorithms are easy to fall into local optimal solution, the hybrid kernel function is constructed and the GWO algorithm is introduced to find the best penalty factor and hybrid coefficient to improve the generalization of the model.

In order to obtain the kernel functions with strong generalization ability, learning ability, and good extrapolation ability, it needs to combine the different kernel functions. The Taylor-Kernel with Moderate Decreasing (T-KMOD) satisfies the zero-point near-descent criterion, with good flexibility, fast

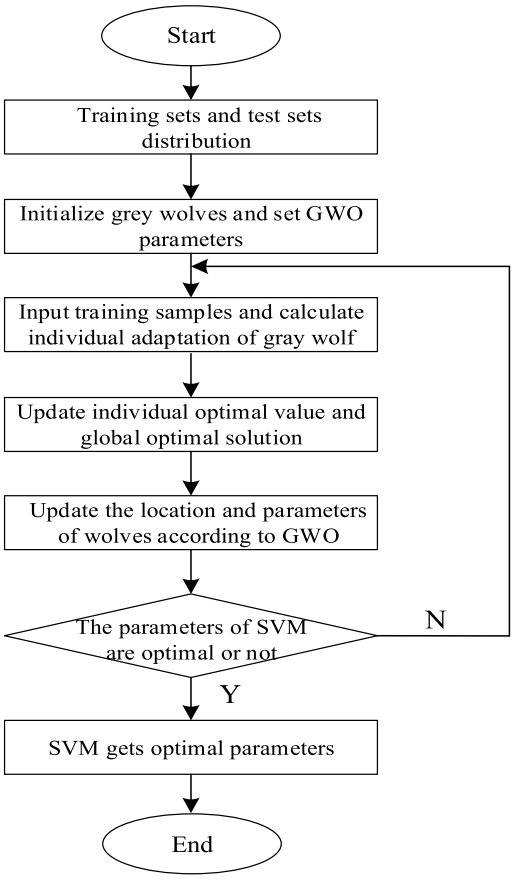

FIGURE 13. Gray wolf optimization algorithm flow chart.

convergence and good locality. Polynomial functions have high classification accuracy and strong generalization ability. Therefore, the two are combined in the following form:

$$S_M = \lambda S_{poly} + (1-\lambda) S_{T-KMOF} \tag{23}$$

where: $S_{T-KMOD} = T - KMOD(x, x') = L\sum_{i=1}^{n}\left(\frac{\gamma}{\|x-x'\|^2+\sigma^2}\right)^{k*i} S_{poly} = [(x\cdot x')+C]^q, \lambda \in (0,1)\ C \geq 0$, $x \cdot x' \in R^n$; L(greater than 0) is used to control the value of the kernel function at 0. σ, γ respectively control the sum and width and the descending speed of the kernel function, and both i and n are positive integers.

GWO has a fast convergence speed, a simple structure, and it is easier to achieve optimal classification. The mathematical model is as follows [24]:

$$\begin{cases} B = \left|C \cdot X_p(t) - X(t)\right| \\ X(t+1) = X_p(t) - A \cdot B \end{cases} \tag{24}$$

where: t represents the current number of iterations; $X_p(t)$ is the prey position vector, and A and C are coefficient vectors. A and C are as follows:

$$\begin{cases} A = 2a \cdot r_1 - a \\ C = 2r_2 \end{cases} \tag{25}$$

where: a is the convergence factor, satisfying $a \in [0, 2]$; r_1 and r_2 are random vectors in [0,1].

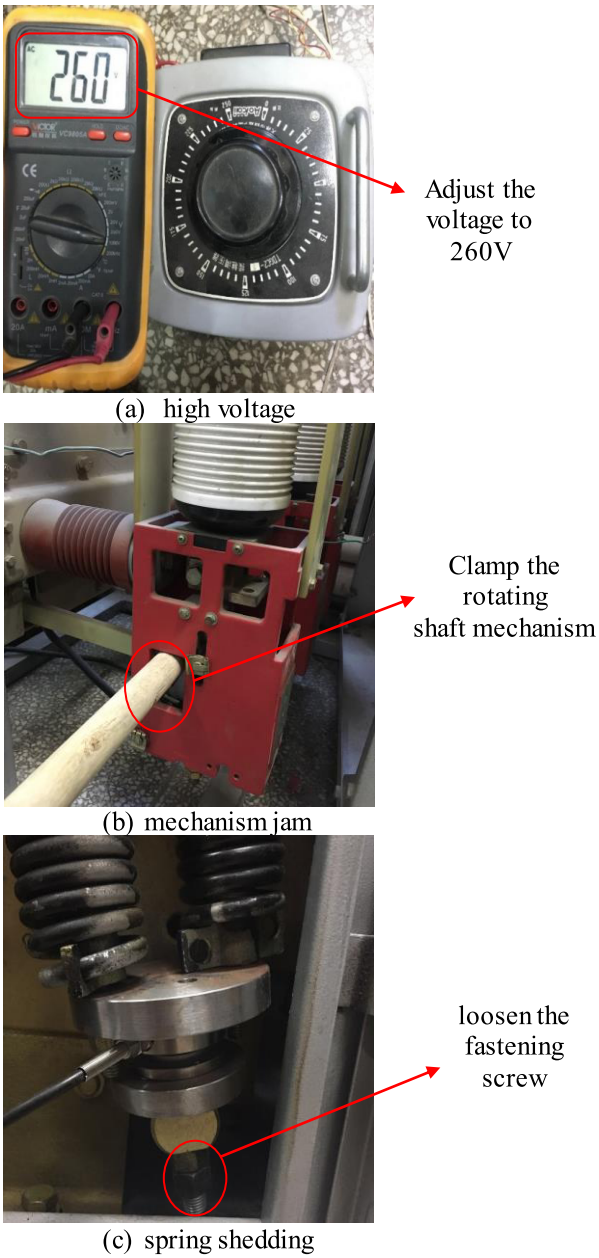

FIGURE 14. Field fault simulation.

Initialize the population, calculate the fitness value of each wolf, select the first three optimal fitness, determine the grey wolf grade, update the location, head wolf, coefficient vectors and other parameters until the SVM parameters are optimal. The flow chart of the algorithm is shown in Fig.13.

B. EXPERIMENTAL RESULT

The sampling rate was set to 40 kHz, 70 sets of samples were collected for each state, 50 sets were used for training, and 20 sets were used for testing. Changing the voltage level in the energy storage process of the circuit breaker can simulate the state of high voltage. The wooden stick is used to clamp the rotating shaft mechanism to increase the damp jamming for simulating mechanism jam. By loosening the fastening screw

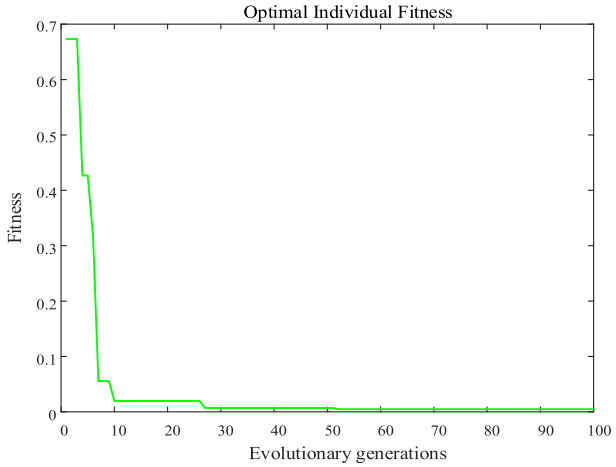

FIGURE 15. The convergence of GWO algorithm.

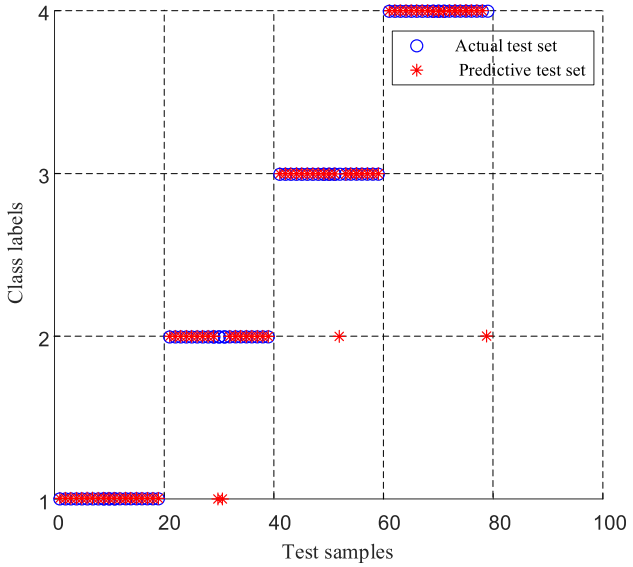

FIGURE 16. Fault identification results of the original SVM model.

at one end of circuit breaker spring can simulated spring shedding. The field test drawings are shown as Fig. 14.

Before using SVM to classify, the parameters of penalty factor C and mixed coefficient λ of SVM need to be optimized. The number of iterations is set to 100, and the optimal parameters are 2.2634 and 0.21, respectively. The convergence of the algorithm is shown in Fig. 15.

Combining Table 1., Table 2. and weight, the current-vibration entropy weight characteristics are constructed. Some test data are shown in Table 4.

The sample label of normal state is set as 1 (group 1-20), the high voltage is 2 (group 21-40), the mechanism jam is 3 (group 41-60), and the spring shedding is 4 (group 61-80). The diagnosis results are as follows. Fig. 16-17 are the fault identification results with the model before and after optimization.

From the results of Fig. 16, it can be seen that the fault identification is carried out by using the current-vibration

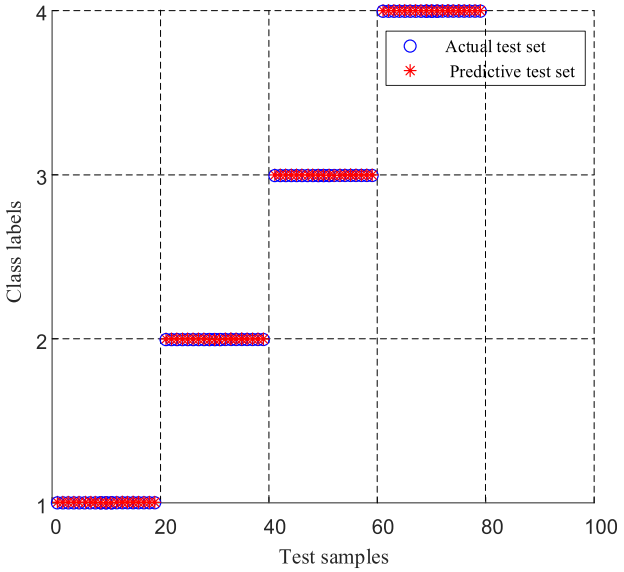

FIGURE 17. Fault identification results of the GWO-SVM model.

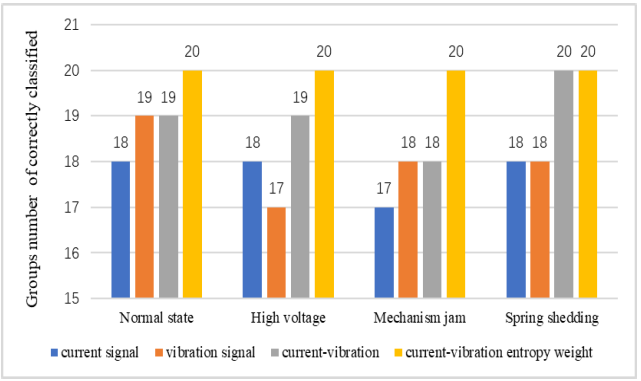

FIGURE 18. Comparison of four feature vectors.

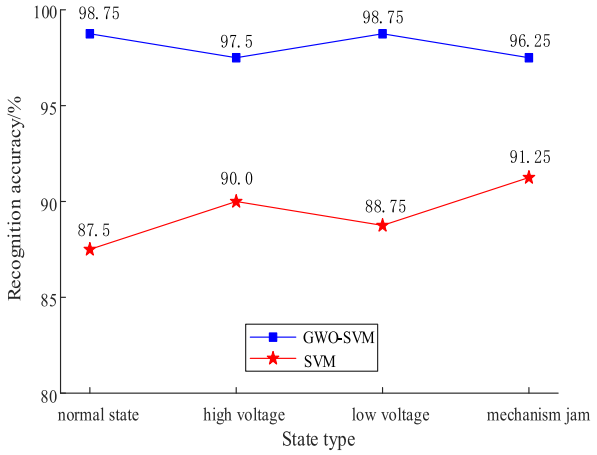

FIGURE 19. Accuracy comparison in four states.

entropy weight characteristic and SVM. The sample labeled 2,3,4 are misclassified, the classification is not very accurate.

The results of GWO-SVM model are shown in Fig.17. All 80 test samples are classified correctly and the identification results are 100%. Therefore, the model can accurately characterize the defect types of energy storage mechanism.

TABLE 4. Testing samples and diagnostic results.

current -vibration entropy weight characteristics												diagnosis label	diagnosis result
I_{st}	I_{sm}	T_{st}	T_{sm}	T_{tal}	K	P_1	P_2	P_3	P_4	P_5	P_6		
0.3221	0.2768	0.0021	0.0733	0.3738	0.4622	0.6252	1.0032	0.7043	0.4545	0.9977	0.1008	1	normal
0.3265	0.2766	0.0019	0.0734	0.3755	0.4603	0.6251	1.0030	0.7040	0.4545	0.9979	0.1008	1	state
0.6083	0.4240	0.0016	0.0811	0.3393	0.4275	0.3737	0.6047	0.4453	0.2782	0.6031	0.0571	2	high
0.6053	0.4242	0.0017	0.0798	0.3245	0.4319	0.3739	0.6048	0.4451	0.2783	0.6033	0.0571	2	voltage
0.3661	0.3102	0.0090	0.1257	0.6324	0.4856	0.5076	0.7100	0.5007	0.3449	0.8021	0.0718	3	mechanism
0.3714	0.3297	0.0088	0.1154	0.6284	0.4987	0.5075	0.7103	0.5009	0.3448	0.8019	0.0718	3	jam
0.3035	0.2326	0.0013	0.0771	0.3872	0.5671	0.1960	0.3284	0.2660	0.1544	0.3211	0.0292	4	spring
0.3020	0.2334	0.0017	0.0759	0.3872	0.5506	0.1961	0.3285	0.2655	0.1545	0.3206	0.0293	4	shedding

C. RESULTS COMPARISON AND ANALYSIS

1) VERIFICATION OF CURRENT-VIBRATION ENTROPY WEIGHT CHARACTERISTIC METHOD

The diagnostic results of current signal, vibration signal, current-vibration combination and current-vibration entropy weight characteristics are compared, as shown in Fig. 18. The diagnostic accuracy rates of current characteristics, vibration characteristics and current-vibration combined characteristics were 88.75%, 90.0% and 95.0% respectively, whereas the diagnostic accuracy of current-vibration entropy weight characteristics reached 100%. It can be concluded that the state information of energy storage mechanism can be reflected more comprehensively based on the current-vibration entropy weight characteristics, and the extracted characteristics are complementary, and the diagnosis effect is improved.

2) GENERALIZED PERFORMANCE VERIFICATION

Due to the different sources and structures of data in the actual operation of high voltage circuit breakers, it is necessary to classify the fault data that the same type with different characterization. In the generalization experiment, the sampling rate is changed from 40 kHz to 30 kHz, and the vibration sensor of PCB357B21 and the current sensor of HCS-LSP are used. At the same time, the position of the sensor is changed. The diagnosis results are shown in Fig.19.

From Fig.19, it's not hard to come out the overall diagnostic accuracy of the GWO-SVM model, it is still 97.8% when the parameters of the acquisition parameters and the type and location of the sensors change, much higher than that of the non-optimal SVM model. This shows that the GWO-SVM model has stronger adaptability to the fresh samples and better generalization ability. But the original current and vibration signals may be different due to the type of circuit breaker and field disturbance. The optimization parameters of VMD and SVM need to be readjusted to adapt to the influence of partial overlap of modal energy spectrum on risk minimization hyperplane partition.

V. CONCLUSION

A new method for identifying abnormal energy storage state of circuit breaker based on current and vibration signal characteristics is proposed. Combining the time-frequency domain entropy weight characteristics of current vibration signal with GWO-SVM optimization algorithm, the accurate identification of multiple faults in different scenarios can be achieved.

1) The motor current and the accompanying vibration signals in the energy storage process are used to diagnose the defects of the energy storage mechanism. Quantitative comparison with the characteristics of the current–vibration signals is a new method for distinguishing the operation state of the energy storage mechanism.

2) K value is selected using the energy method and α is selected using objective function optimization method. The vibration signal is decomposed by using VMD to obtain permutation entropy of the modal components, thus quantitatively characterizing the frequency domain distribution of the vibration signal.

3) Envelope denoising in the modulus maxima wavelet domain and HT are combined to improve feature extraction accuracy of current in time domain.

4) The operation state of the energy storage mechanism of the circuit breaker from the angle of information entropy is reflected by constructing current–vibration entropy weight characteristics, which can improve the accuracy rate of circuit breaker energy storage mechanism fault diagnosis.

5) A diagnosis model based on GWO–SVM, which greatly improves the accuracy and generalization of model identification and has broad application value, is proposed.

REFERENCES

[1] A. A. Razi-Kazemi, M. Vakilian, K. Niayesh, and M. Lehtonen, "Circuit-breaker automated failure tracking based on coil current signature," *IEEE Trans. Power Delivery*, vol. 29, no. 1, pp. 283–290, Feb. 2014.
[2] Z. Shutao, Z. Pei, S. Lu, and G. Jing, "Vibration and acoustic joint mechanical fault diagnosis method of high voltage circuit breakers," *Trans. China Electrotech. Soc.*, vol. 29, no. 7, pp. 216–221, 2014.
[3] Y. W. Yang, Y. G. Guan, and S. G. Chen, "Mechanical fault diagnosis method of high voltage circuit breaker based on sound signal," *Proc. CSEE.*, vol. 38, no. 22, pp. 6730–6737, 2018.
[4] Q. Yang, J. Ruan, Z. Zhuang, D. Huang, and Z. Qiu, "A new vibration analysis approach for detecting mechanical anomalies on power circuit breakers," *IEEE Access*, vol. 7, pp. 14070–14080, 2019.
[5] M. Landry, F. Leonard, C. Landry, R. Beauchemin, O. Turcotte, and F. Brikci, "An improved vibration analysis algorithm as a diagnostic tool for detecting mechanical anomalies on power circuit breakers," *IEEE Trans. Power Del.*, vol. 23, no. 4, pp. 1986–1994, Oct. 2008.
[6] L. P. Zhang, D. Y. Shi, and X. R. Miu, "Research on vibration signal feature analysis and its fault diagnosis," *Electro Mach. Control*, vol. 20, no. 10, pp. 82–87, 2016.

[7] J. S. Smith, "The local mean decomposition and its application to EEG perception data," *J. Roy. Soc. Interface*, vol. 2, no. 5, pp. 443–454, 2005.
[8] W. Sun, B. S. Xiong, and J. P. Huang, "Rolling bearing fault diagnosis method combining wavelet packet noise reduction and LMD," *Vib. Impact.*, vol. 31, no. 18, pp. 153–156, 2012.
[9] S. S. Li, F. H. Wang, and Q. J. Geng, "Mechanical state detection of high voltage circuit breakers based on optimized VMD," *Electric Power Autom. Equip.*, vol. 38, no. 11, pp. 148–154, 2018.
[10] S. Tian and Z. H. Kang, "Mechanical fault diagnosis analysis of 10 kV high voltage circuit breaker based on VMD algorithm," *Power Sci. Eng.*, vol. 34, no. 6, pp. 73–78, 2018.
[11] Z. B. Qiu, J. J. Ruan, and D. C. Huang, "Mechanical fault diagnosis of high voltage disconnector based on motor current detection," *Proc. CSEE.*, vol. 35, no. 13, pp. 3459–3466, 2015.
[12] M. Runde, T. Aurud, L. E. Lundgaard, G. E. Ottesen, and K. Faugstad, "Acoustic diagnosis of high voltage circuit-breakers," *IEEE Trans. Power Del.*, vol. 7, no. 3, pp. 1306–1315, Jul. 1992.
[13] J. L. Yuan, K. Li, and Z. T. Guo, "Mechanical fault diagnosis of high voltage circuit breakers based on SVM and current parameters of closing and closing coils," *High Voltage Electroal Appliances*, vol. 47, no. 3, pp. 26–30, 2011.
[14] K. Zhao, F. Wang, and Y. W. Yang, "Mechanical state evaluation of high voltage circuit breakers based on signal feature fusion and optimization," *High Voltage Electroal Appliances*, vol. 54, no. 4, pp. 14–19, 2018.
[15] Z. C. Yang, C. L. Zhang, and L. G. Ge, "Comprehensive fuzzy evaluation based on entropy weight method for insulator flashover pollution," *Electro Power Autom. Equipment.*, vol. 34, no. 4, pp. 90–94, 2014.
[16] S. G. Sun, L. Y. Zhao, and T. H. Du, "Mechanical fault diagnosis of universal circuit breaker based on motor current analysis," *J. Instrum. Instrum.*, vol. 38, no. 4, pp. 952–960, 2017.
[17] T. Y. Xu, Z. L. Pu, and C. L. Chen, "Hilbert transform and wavelet denoising improve the accuracy of transient power quality disturbance detection and location," *J. Agricult. Eng.*, vol. 28, no. 19, pp. 150–155, 2012.
[18] X. F. Zhang, D. Z. Xu, and Z. F. Qi, "Research on denoising algorithm based on modulus maxima wavelet domain," *Data Acquisition Process.*, vol. 18, no. 3, pp. 315–318, 2003.
[19] C. Wang, H. Li, G. Huang, and J. Ou, "Early fault diagnosis for planetary gearbox based on adaptive parameter optimized VMD and singular kurtosis difference spectrum," *IEEE Access*, vol. 7, pp. 31501–31516, 2019.
[20] C. Bandt and B. Pompe, "Permutation entropy: A natural complexity measure for time series," *Phys. Rev. Lett.*, vol. 88, no. 17, 2002, Art. no. 174102.
[21] A. M. Fraser and H. L. Swinney, "Independent coordinates for strange attractors from mutual information," *Phys. Rev. A, Gen. Phys.*, vol. 33, no. 2, pp. 1134–1140, Feb. 1986.
[22] P. Grassberger and I. Procaccia, "Characterization of strange attractors," *Phys. Rev. Lett.*, vol. 50, no. 5, p. 346, Jan. 1983.
[23] S. Ouyang and Y. L. Shi, "Improved entropy weight method and its application in power quality assessment," *Power Syst. Automat.*, vol. 37, no. 21, pp. 156–159, 2013.
[24] S. Mirjalili, S. M. Mirjalili, and A. Lewis, "Grey wolf optimizer," *Adv. Eng. Softw.*, vol. 69, pp. 46–61, Mar. 2014.

SHUTAO ZHAO was born in 1968. He received the bachelor's degree from the University of Electronic Science and Technology, in 1990, and the master's and Ph.D. degrees in electrical theory and new technology from North China Electric Power University, in 1999 and 2006, respectively, where he is currently a Professor. His research interests include online monitoring, electrical equipment fault diagnosis, and modern electromagnetic measurement technology. He also serves as the Director of the Electromagnetic Measurement Branch, Chinese Instrument and Instrument Society.

ERXU WANG was born in Baoding, Hebei, in 1994. He received the bachelor's degree in power system automation from North China Electric Power University, in 2017, where he is currently pursuing the master's degree.

His research interests include online monitoring, electrical equipment fault diagnosis, and signal processing technology.